α1-Syntrophin–deficient skeletal muscle exhibits hypertrophy and aberrant formation of neuromuscular junctions during regeneration

Yukio Hosaka,[1,2] Toshifumi Yokota,[1,3] Yuko Miyagoe-Suzuki,[1] Katsutoshi Yuasa,[1] Michihiro Imamura,[1] Ryoichi Matsuda,[4] Takaaki Ikemoto,[5] Shuhei Kameya,[6] and Shin'ichi Takeda[1]

[1]Department of Molecular Therapy, National Institute of Neuroscience, National Center of Neurology and Psychiatry, Kodaira 187-8502, Tokyo, Japan
[2]Department of Neurology, Nakadori General Hospital, Akita 010-8577, Japan
[3]Department of Biological Sciences, Graduate School of Science, The University of Tokyo, Tokyo 113-8654, Japan
[4]Department of Life Sciences, Graduate School of Arts and Sciences, The University of Tokyo, Tokyo 153-8902, Japan
[5]Department of Pharmacology, Saitama Medical School, Moroyama-machi, Saitama 350-0495, Japan
[6]Department of Ophthalmology, Akita University, Akita 010-8543, Japan

α1-Syntrophin is a member of the family of dystrophin-associated proteins; it has been shown to recruit neuronal nitric oxide synthase and the water channel aquaporin-4 to the sarcolemma by its PSD-95/SAP-90, Discs-large, ZO-1 homologous domain. To examine the role of α1-syntrophin in muscle regeneration, we injected cardiotoxin into the tibialis anterior muscles of α1-syntrophin–null (α1syn$^{-/-}$) mice. After the treatment, α1syn$^{-/-}$ muscles displayed remarkable hypertrophy and extensive fiber splitting compared with wild-type regenerating muscles, although the untreated muscles of the mutant mice showed no gross histological change. In the hypertrophied muscles of the mutant mice, the level of insulin-like growth factor-1 transcripts was highly elevated. Interestingly, in an early stage of the regeneration process, α1syn$^{-/-}$ mice showed remarkably deranged neuromuscular junctions (NMJs), accompanied by impaired ability to exercise. The contractile forces were reduced in α1syn$^{-/-}$ regenerating muscles. Our results suggest that the lack of α1-syntrophin might be responsible in part for the muscle hypertrophy, abnormal synapse formation at NMJs, and reduced force generation during regeneration of dystrophin-deficient muscle, all of which are typically observed in the early stages of Duchenne muscular dystrophy patients.

Introduction

Syntrophins are 58–60 kD peripheral membrane proteins that have been shown to bind to COOH-terminal domains of dystrophin, utrophin, dystrobrevins, and their shorter isoforms (Cartaud et al., 1993; Kramarcy et al., 1994; Ahn and Kunkel, 1995; Suzuki et al., 1995; Yang et al., 1995). To date, five isoforms, α1-, β1-, β2-, γ1-, and γ2-syntrophins, have been identified (Adams et al., 1993; Ahn et al., 1994; Piluso et al., 2000). All five syntrophins have a similar domain structure: two pleckstrin homology domains, a PSD-95/SAP-90, Discs-large, ZO-1 homologous (PDZ)* domain, and a syntrophin unique domain (Adams et al., 1995; Piluso et al., 2000), predicting multiple roles in anchoring proteins at the membrane through the PDZ domain and in signal transduction. α1-Syntrophin is expressed mainly in skeletal muscle, cardiac muscle, and brain. In skeletal muscle, it is expressed both at the sarcolemma and the neuromuscular junctions (NMJs). α1-Syntrophin interacts with dystrophin at the extrajunctional sarcolemma, whereas it also associates with utrophin on the crests and with dystrophin in the depths of the junctional folds at NMJs (Byers et al., 1991; Sealock et al., 1991). Adams et al. (2000) have reported that

Address correspondence to Shin'ichi Takeda, National Institute of Neuroscience, National Center of Neurology and Psychiatry, 4-1-1 Ogawa-higashi, 187-8502 Kodaira, Tokyo, Japan. Tel.: 81-42-346-1720. Fax: 81-42-346-1750. E-mail: takeda@ncnp.go.jp

Y. Hosaka and T. Yokota contributed equally to this work.

*Abbreviations used in this paper: α1syn$^{-/-}$, α1-syntrophin–null; α-BgTx, α-bungarotoxin; AChR, acetylcholine receptor; AQP4, aquaporin-4; CSA, cross-sectional area; DMD, Duchenne/Becker muscular dystrophy; G3PDH, glyceraldehyde-3-phosphate dehydrogenase; IGF, insulin-like growth factor; nNOS, neuronal nitric oxide synthase; MHC, myosin heavy chain; NMJ, neuromuscular junction; PDZ, PSD-95/SAP-90, Discs-large, ZO-1 homologous domain; TA, tibialis anterior; VGSC, voltage-gated sodium channel.

Key words: α1-syntrophin; skeletal muscle; hypertrophy; regeneration; neuromuscular junction

α1-syntrophin–deficient mice have shallow nerve gutters, abnormal distribution of acetylcholine receptors (AChRs), and less organized postjunctional folds. However, the mutant mice have no deficiency in their ability to exercise (Adams et al., 2000). Although the function of α1-syntrophin is not fully understood, the PDZ domain of α1-syntrophin is known to interact with several molecules. Brenman et al. (1996) reported the interaction of α1-syntrophin with neuronal nitric oxide synthase (nNOS) in skeletal muscle. More recently, we demonstrated the loss of nNOS from the sarcolemma in α1-syntrophin–null (α1syn$^{-/-}$) muscle (Kameya et al., 1999). Interestingly, the α1syn$^{-/-}$ skeletal muscle was not dystrophic and showed similar contractile properties to those of control muscles (Kameya et al., 1999). These results suggested that the loss of sarcolemmal nNOS is not directly responsible for muscle degeneration in dystrophin-deficient muscular dystrophy. We have reported that α1-syntrophin also plays a major role in recruiting aquaporin-4 (AQP4), a water channel, to the sarcolemma in vivo (Yokota et al., 2000). However, we have observed no direct interaction between AQP4 and α1-syntrophin in vitro, suggesting the intervention of as yet unrecognized proteins. In dystrophin-deficient muscular dystrophy, the loss of dystrophin causes secondary loss of dystrophin-associated proteins, including α- and β-dystroglycans, α-, β-, γ-, and δ-sarcoglycans, sarcospan, dystrobrevins, and α1- and β1-syntrophins, from the sarcolemma (for review see Ozawa et al., 1995). Therefore, the degeneration/regeneration process, which occurs throughout the course of the disease, is greatly modified by the loss of many other functional molecules. In this respect, molecular dissection of the dystrophin complex is required to understand the molecular pathogenesis of Duchenne/Becker muscular dystrophy (DMD). It is a well-known characteristic of DMD that regeneration is not sufficient to compensate for the fiber breakdown that occurs throughout the course of the disease. Whether the lack of dystrophin and reduced levels of associated proteins directly affect the ability of fibers of DMD to regenerate is unclear (Cullen, 1997). To clarify the roles of α1-syntrophin in muscle regeneration, we injected cardiotoxin into the tibialis anterior (TA) muscles of wild-type and α1syn$^{-/-}$ mice. Cardiotoxin is known to damage the plasma membrane of myofibers but leave basal lamina, satellite cells, and nerves intact, allowing rapid and reproducible muscle regeneration. Toxin-treated muscles of α1syn$^{-/-}$ mice were significantly hypertrophied at 2–8 wk after injection. Furthermore, the ability to exercise and contractile properties of regenerating muscle of the mutant mice were considerably impaired. In addition, α1syn$^{-/-}$ mice had aberrant NMJs from an early stage of regeneration. These results suggest that the absence of α1-syntrophin resulted in aberrant synapse formation at NMJs, reduction of contractile force, and muscle hypertrophy.

Results

The early phase of muscle regeneration of α1syn$^{-/-}$ mice

To clarify the roles of α1-syntrophin in muscle regeneration, we injected cardiotoxin into TA muscles of wild-type and α1syn$^{-/-}$ mice and then examined the process of regeneration at various times after injection (from 1 d to 12 wk). Hematoxylin and eosin staining of TA muscles showed that muscle regeneration of α1syn$^{-/-}$ mice was indistinguishable from that of the wild-type for up to 2 wk after cardiotoxin injection. There was no significant difference in the expression of myogenic helix-loop-helix transcription factors (MyoD, myf5, myogenin, and myf6), dystrophin, myosin heavy chains (MHCs) (embryonic, neonatal, type I, IIa, IIb, IIx), or laminin-α2 chain between toxin-injected muscles of α1syn$^{-/-}$ mice and those of wild-type mice (unpublished data).

Hypertrophy and extensive fiber splitting of α1syn$^{-/-}$ regenerating TA muscles at 2–8 wk after cardiotoxin treatment

From 2 wk after injection, regenerating TA muscles of α1syn$^{-/-}$ mice were much larger than regenerating wild-type TA muscles (Fig. 1 a). The relative weight of regenerating α1syn$^{-/-}$ TA muscles was much increased at 2, 4, 8, and 12 wk after cardiotoxin injection compared with those of wild-type muscles. The relative weight of the untreated TA muscle to body weight of α1syn$^{-/-}$ and wild-type mice was constant, regardless of sex or age.

The numbers of myofibers are significantly increased in cardiotoxin-injected muscle of α1syn$^{-/-}$ mice

To determine whether the increase of muscle weight of α1syn$^{-/-}$ regenerating muscle reflects hyperplasia or hypertrophy of each fiber, the total number of myofibers in a cross section of TA muscles was counted (Fig. 1 b). In untreated left TA muscles, there was no difference in the total number of muscle fibers between α1syn$^{-/-}$ and wild-type mice. However, the number of fibers after cardiotoxin treatment was much higher in α1syn$^{-/-}$ muscle than in wild-type muscle ($P < 0.05$), although the numbers of fibers increased even in the wild-type muscle after the treatment. As shown in Fig. 2, the increase in numbers of muscle fibers was thought to be due to excessive and extensive fiber splitting. Typical fiber splitting was found in a hypertrophied fiber with several central nuclei (Fig. 2 h). In transverse sections through the midportion of the TA muscle, we compared the size of TA muscles at each time of sampling. Fig. 2 shows representative images of noninjected and cardiotoxin-injected muscles of wild-type and α1syn$^{-/-}$ mice at 4 wk after injection. In untreated muscles, there was no apparent difference in the size of transverse sections between noninjected muscles of wild-type (Fig. 2 a) and α1syn$^{-/-}$ mice (Fig. 2 b), but the size of α1syn$^{-/-}$ cardiotoxin-treated muscle (Fig. 2 d) was much larger than that of wild-type toxin-injected muscle (Fig. 2 c). High power magnification revealed many large caliber fibers and marked fiber splitting in the α1syn$^{-/-}$ cardiotoxin-injected muscles (Fig. 2 h). In wild-type regenerating muscles, hypertrophic fibers were less frequent, and fiber splitting was mild (Fig. 2 g).

Type IIb muscle fibers were preferentially hypertrophied in regenerating muscles of α1syn$^{-/-}$ mice

To examine the relation between fiber types (IIa, IIb, or IIx type fibers) and hypertrophy or fiber splitting, we next classified the muscle fibers by their expression of MHC isoforms

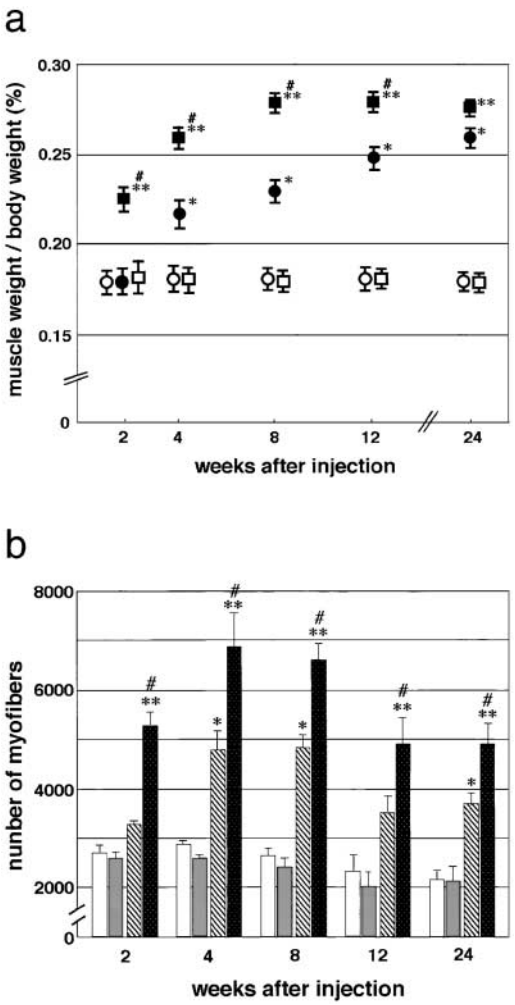

Figure 1. **Changes in the weight and the number of myofibers in TA muscles after cardiotoxin injection.** (a) The weight of TA muscle was normalized to body weight. Relative weight of regenerating α1syn$^{-/-}$ TA muscles to body weight is significantly increased at 2, 4, 8, and 12 wk after cardiotoxin injection compared with that of regenerating wild-type muscles. Values are mean ± SEM for 4–10 muscles/group. #Significant difference ($P < 0.05$) between cardiotoxin-injected muscles of α1syn$^{-/-}$ (■) and wild-type (●) mice. *Significant difference ($P < 0.05$) between noninjected (○) and toxin-injected muscles (●) of wild-type mice. **Significant difference ($P < 0.05$) between noninjected (□) and toxin-injected (■) muscles of α1syn$^{-/-}$ mice. There was no significant difference between untreated muscles of wild-type (○) and α1syn$^{-/-}$ mice (□). (b) Changes in the number of myofibers in TA muscles after cardiotoxin injection. There was no significant difference between untreated muscles of wild-type (white bars) and α1syn$^{-/-}$ mice (grey bars), whereas the ratio of increase in the numbers of fibers after cardiotoxin treatment was much higher in α1syn$^{-/-}$ muscle than in wild-type muscle. Values are mean ± SEM for three to six muscles/group. *Significant difference ($P < 0.05$) from untreated muscles of wild-type mice. #Significant difference ($P < 0.05$) between untreated and cardiotoxin-injected muscles (black bars) of α1syn$^{-/-}$ mice. **Significant difference ($P < 0.05$) from cardiotoxin-injected muscles (hatched bars) of wild-type mice.

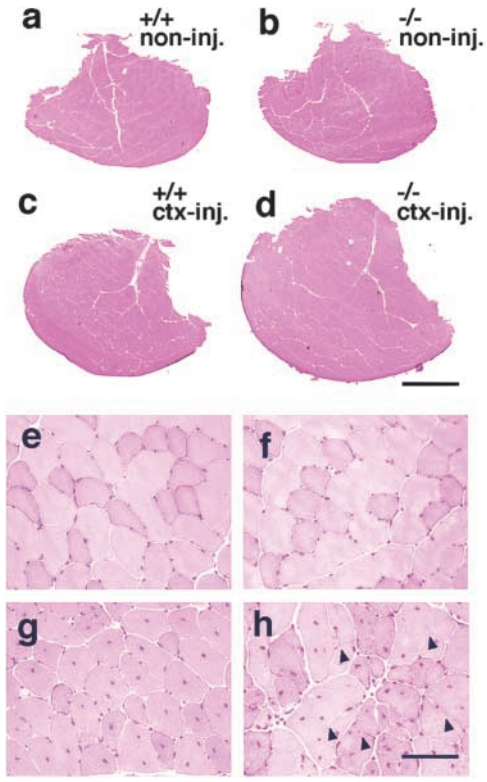

Figure 2. **Histology of α1syn$^{-/-}$ TA muscle afer carditoxin injection.** The largest CSA of TA muscles removed from mice of approximately the same body weight at 4 wk after cardiotoxin injection. (a–d) Untreated contralateral muscle of wild-type (a) and α1syn$^{-/-}$ (b) mice. Cardiotoxin-injected muscle of wild-type (c) and α1syn$^{-/-}$ (d) mice. The size of α1syn$^{-/-}$ cardiotoxin-treated muscle is much larger than that of wild-type toxin-injected muscle, although there was no apparent difference between noninjected muscle of wild-type and α1syn$^{-/-}$ mice. High power magnification view of each muscle (e–h). Noninjected muscle of wild-type (e) and α1syn$^{-/-}$ mice (f). Cardiotoxin-injected muscle of wild-type mice (g).Cardiotoxin-injected muscle of α1syn$^{-/-}$ mice (h) displayed many large caliber fibers and fiber splitting (arrowheads). Bars: (a–d) 1 mm; (e–h) 50 μm.

using MHC isoform-specific antibodies. In the TA muscle, a few fibers expressing slow type MHC I were found mainly in the central part of the TA muscle. At 2 or 4 wk after toxin injection, no muscle fiber expressed embryonic/neonatal MHCs (unpublished data). Next, we separately measured the cross-sectional area (CSA) of each fiber in the central or marginal part of cardiotoxin-injected or untreated TA muscles. Fig. 3 shows the frequency distribution of fiber CSAs in the marginal part of TA muscle at 4 wk after cardiotoxin injection. There was no significant difference in either average or standard deviation of CSA between untreated wild-type and α1syn$^{-/-}$ muscles. However, in regenerating muscle, the mean CSA in the α1syn$^{-/-}$ muscle was much larger than that of the wild-type muscle from 2 wk after cardiotoxin injection. Although the mean CSA of α1syn$^{-/-}$ regenerating muscles was equal to that of contralaterals, the fiber size distribution was significantly different at 4 wk after injection. There were many large caliber fibers that were not detected in untreated contralateral TA muscles, together with many small caliber fibers. These large or small caliber muscle fibers were often found in the marginal area. Fig. 3 demonstrates that these fibers were IIb or IIx type fibers. On the other hand, the fiber size distribution of IIa type was not significantly different between genotypes. In wild-type regenerating muscles, the diversion of CSA was higher from contralaterals, but hypertrophied fibers were less numerous than

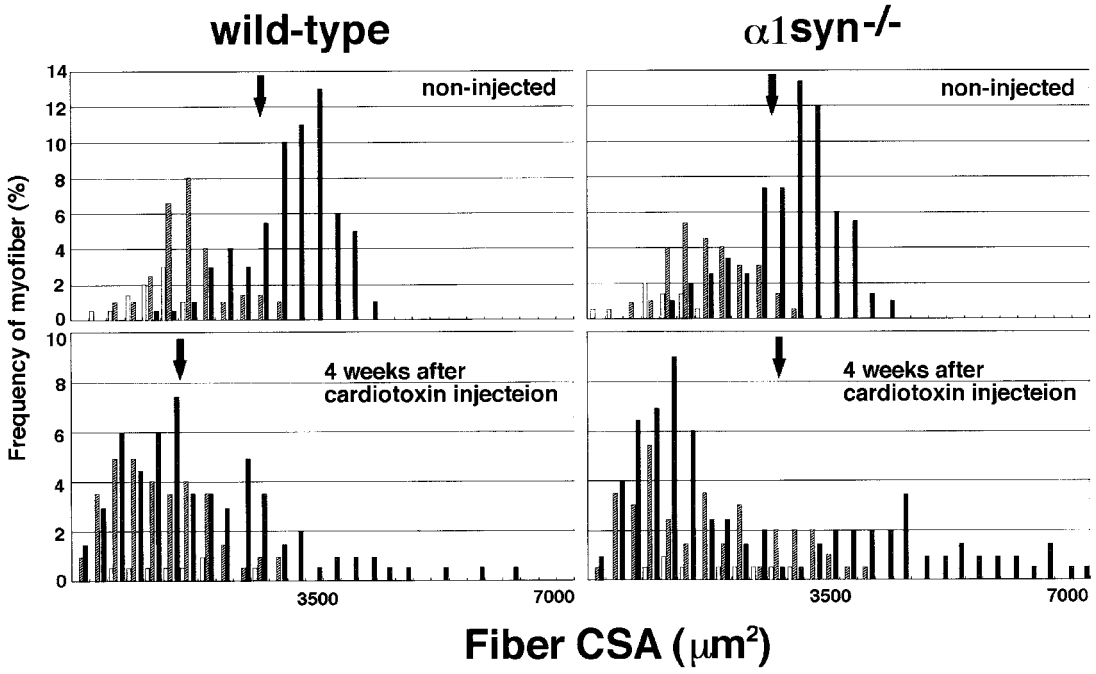

Figure 3. **Frequency distribution of the fiber CSA in TA muscle at 4 wk after cardiotoxin injection.** A total of 200 fiber profiles were traced in each section for three muscles from mice of approximately the same body weight. Each fiber was classified by the expression of MHC IIa (white bars), MHC IIx (hatched bars), or MHC IIb (black bars) isoform. Arrow shows the mean of fiber CSA.

in α1syn$^{-/-}$ toxin–injected muscles. The mean in wild-type toxin-injected muscles was much smaller than contralaterals at 4 wk after injection.

The shift of MHC isoform expression in skeletal muscle from α1syn$^{-/-}$ mice during regeneration

To identify the fiber type in the regenerating muscle of the mutant mice quantitatively, we examined the MHC isoform composition in skeletal muscle from α1syn$^{-/-}$ mice during regeneration using 8% polyacrylamide gel containing glycerol. Although there was no gross difference between the proportions of MHC isoforms in the untreated wild-type and mutant muscles, the level of MHC IIa was significantly lower at 7 d after the cardiotoxin injection compared with that of wild-type muscle (Fig. 4 a). In contrast, MHC IIb and IIx levels were slightly higher in the mutant mice at this stage. In the mutant mice, although the MHC isoform composition shifted from slow to fast type at 7 d, they returned to the same levels as control mice 4–8 wk after the injection. At 7 d after the treatment, narrow bands corresponding to MHC neonatal were also detected between MHC IIx and IIb in both the wild-type and mutant lanes, but they were not significantly different between genotypes. The results were shown in Table I.

The level of insulin-like growth factor-1 mRNA was elevated in regenerating muscles

Because there were many hypertrophied fibers in regenerating TA muscle of α1syn$^{-/-}$ mice, we investigated whether insulin-like growth factor (IGF)-1 was involved in muscle hypertrophy of α1syn$^{-/-}$ mice. We examined the expression of IGF-1 mRNA in regenerating TA muscles at 2 and 4 wk after the toxin injection (Fig. 5). In untreated muscles, there was no significant difference in the expression of IGF-1 mRNA between α1syn$^{-/-}$ and wild-type mice. In contrast, the levels of IGF-1 transcripts in regenerating muscles of α1syn$^{-/-}$ at 2 and 4 wk after cardiotoxin injection were significantly higher than those of wild-type mice, suggesting IGF-1 may be one of the major factors which induce hypertrophy in regenerating mutant muscle. In wild-type mice, the IGF-1 mRNA level was elevated at 2 wk but had returned to the control level at 4 wk after injection.

Table I. **Relative MHC protein content of regenerating TA muscle in wild-type and α1syn$^{-/-}$ mice**

	Wild-type				α1syn$^{-/-}$			
Group	**Noninjected**	**1 wk**	**4 wk**	**8 wk postinjection**	**Noninjected**	**1 wk**	**4 wk**	**8 wk postinjection**
Type I	0.54 ± 0.42	0.81 ± 0.72	0.12 ± 0.12	0.20 ± 0.20	0.00 ± 0.00	0.20 ± 0.20	0.03 ± 0.02	0.00 ± 0.00
Type IIa	0.00 ± 0.00	6.33 ± 0.50	0.33 ± 0.33	0.02 ± 0.02	0.00 ± 0.00	1.37 ± 1.37[a]	0.00 ± 0.00	0.00 ± 0.00
Type IIx	31.78 ± 0.36	29.03 ± 1.13	38.72 ± 1.47	31.58 ± 0.15	32.38 ± 0.43	33.54 ± 1.61	38.91 ± 2.58	31.62 ± 0.67
Type IIb	67.67 ± 0.63	63.83 ± 1.57	60.48 ± 1.19	68.20 ± 0.05	67.62 ± 1.44	64.89 ± 2.30	60.83 ± 2.58	68.38 ± 0.53

Values are mean ± SEM. n = 3–7 for each group.
[a]$P < 0.05$ compared with ctx-injected TA muscles of wild-type mice by Student's t test.

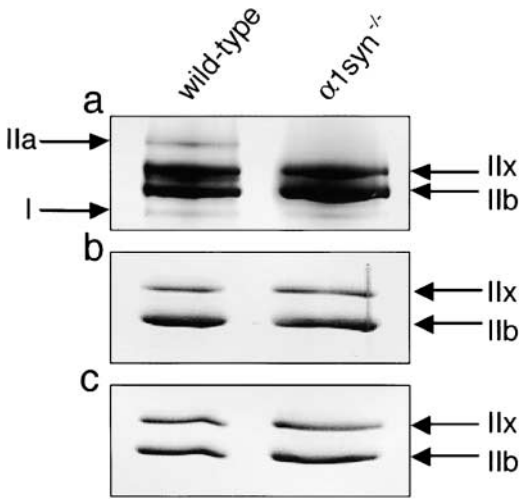

Figure 4. **MHC contents in wild-type and α1syn$^{-/-}$ regenerating TA muscles.** Electrophoretic separation of wild-type and α1syn$^{-/-}$ TA muscle MHCs at 7 d (a) and 4 wk (b) after cardiotoxin injection, and nontreated muscle (c). Representative silver-stained SDS–polyacrylamide gel shows a significantly lower level of MHC IIa and slightly higher levels of IIb and IIx in α1syn$^{-/-}$ muscle at 7 d after injection.

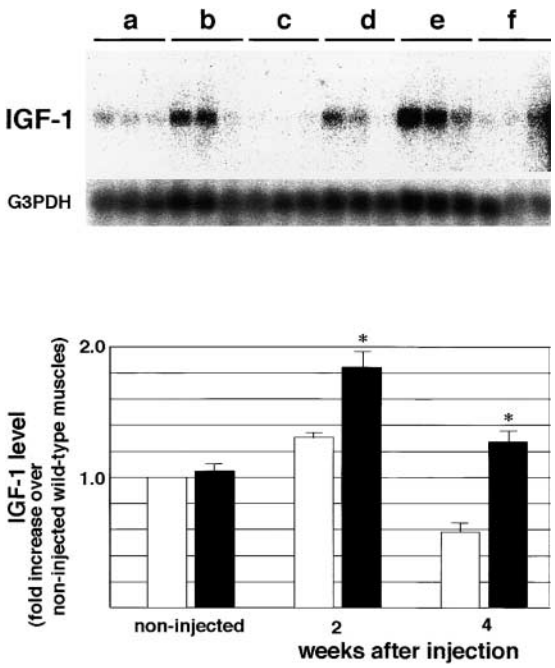

Figure 5. **Changes in IGF-1 mRNA level in TA muscles after cardiotoxin injection.** The top panel shows the IGF-1 mRNA Northern blot analysis for three muscles/group. G3PDH mRNA was used as a control. RNA was obtained from noninjected (a) and cardiotoxin-injected muscles of wild-type mice at 2 wk (b) and 4 wk (c) after injection. Untreated (d) and cardiotoxin-injected muscles of α1syn$^{-/-}$ mice at 2 wk (e) and 4 wk (f) after injection were also analyzed. The bottom panel shows the increase of IGF-1 mRNA over untreated wild-type muscles. IGF-1 mRNA level was normalized to G3PDH mRNA level. Values are mean ± SEM for four samples/group. *Significant difference ($P < 0.05$) between wild-type (white bars) and α1syn$^{-/-}$ mice (black bars).

α1-Syntrophin–deficient mice were impaired in exercise endurance in the early phase of regeneration

To test the exercise endurance of α1syn$^{-/-}$ mice during the aberrant muscle regeneration process, we employed a wire net holding test (Fig. 6). Although all untreated mice of both wild-type and α1syn$^{-/-}$ mice completed a maximum holding time of 5 min in the test (Fig. 6 a), the time of α1syn$^{-/-}$ male mice (38.1 ± 15.2 s) was significantly shorter ($P < 0.05$) than that of wild-type male mice (151.0 ± 38.2 s) at 7 d after cardiotoxin injection (Fig. 6 b). α1syn$^{-/-}$ female mice showed almost the same fatigability as male mice. We could not detect any difference between genotypes at a later time point (4–8 wk after treatment) (unpublished data).

Tetanic force and isomeric twitch force were much reduced in the regenerating muscles of α1syn$^{-/-}$ mice

To test the hypothesis that hypertrophy of regenerating α1syn$^{-/-}$ muscle might be related to reduced force production, we next examined the maximal tetanic force and the peak twitch force of α1syn$^{-/-}$ and wild-type regenerating muscles at 4 wk after cardiotoxin injection. The results are summarized in Table II. Although the specific tetanic force and the specific twitch force of α1syn$^{-/-}$ untreated muscle were not significantly different from those of wild-type control muscle, those of α1syn$^{-/-}$ regenerating muscle were significantly reduced compared with those of untreated muscles.

Table II. **Contractile force of TA muscles at 4 wk after ctx injection**

	Wild-type		α1syn$^{-/-}$	
Parameter	**Noninjected**	**Injected**	**Noninjected**	**Injected**
L_0, mm	11.82 ± 0.53	11.19 ± 0.37	11.15 ± 0.44	11.01 ± 0.47
TA weight, mg	15.40 ± 1.10	17.10 ± 1.56	14.71 ± 1.20	17.95 ± 1.28[a]
TA CSA, mm^2	1.23 ± 0.05	1.38 ± 0.08	1.27 ± 0.12	1.56 ± 0.11[a,b]
Twitch force, mN	43.75 ± 10.01	69.55 ± 14.13[a]	41.89 ± 5.10	35.32 ± 4.51[c]
Tetanic force, mN	145.29 ± 32.67	217.59 ± 32.18[a]	140.90 ± 18.05	127.72 ± 14.91[c]
Specific twitch force, mN/mm^2	35.57 ± 8.14	50.40 ± 10.24	33.00 ± 4.02	22.64 ± 2.89[a,c]
Specific tetanic force, mN/mm^2	118.01 ± 28.25	161.17 ± 23.84[a]	110.95 ± 16.09	79.95 ± 10.89[a,c]

Values are mean ± SEM. n = 5–8 for each group.
[a]$P < 0.05$ compared with contralateral noninjected TA muscles.
[b]$P < 0.01$.
[c]$P < 0.001$ compared with ctx-injected TA muscles of wild-type mice by Mann-Whitney's U test.

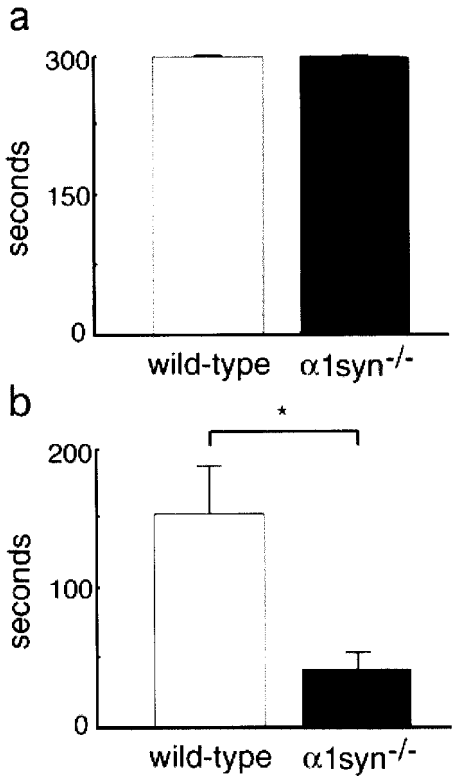

Figure 6. **Impaired ability of α1syn$^{-/-}$ mice in wire net holding test at 7 d after cardiotoxin injection.** Maintenance time in the test of untreated mice (a) or cardiotoxin-injected mice (b) at 7 d after the treatment. α1syn$^{-/-}$ mice are impaired in their ability to perform the exercise at the early stage of the regeneration process. Values are mean ± SEM. *Significant difference ($P < 0.05$) between cardiotoxin-injected mice of α1syn$^{-/-}$ and wild-type.

α1syn$^{-/-}$ skeletal muscle showed aberrant NMJs in the regeneration process

Since α1-syntrophin is strongly expressed at NMJs (Peters et al., 1997), we examined the morphology and utrophin expression at NMJs in α1syn$^{-/-}$ skeletal muscle in regeneration. Alexa 594–labeled α-bungarotoxin (α-BgTx) was used to identify NMJs. Regenerating TA muscle of α1syn$^{-/-}$ mice had remarkably shallow nerve gutters at NMJs, although the untreated mutant mice showed moderate abnormality (Fig. 7). Interestingly, the localization of utrophin in the mutant mice (Fig. 7 p) was not completely coincident with that of AChR (Fig. 7 q), especially at 8 wk after injection.

Expression of α1-syntrophin, β1-syntrophin, neuronal NOS, AQP4, voltage-gated sodium channel, caveolin-3, and α-dystrobrevin in muscle regeneration of wild-type and α1syn$^{-/-}$ mice

α1-Syntrophin has been reported to interact with several signaling molecules or channels. To clarify whether these molecules are involved in the mechanism of force deficit and hypertrophy seen in α1syn$^{-/-}$ regenerating muscle, we examined the expression of these molecules during regeneration. In wild-type mice, sarcolemmal expression of α1-syntrophin was detected in muscles of untreated mice and at 4 wk after cardiotoxin injection (Fig. 8, a and b). In α1syn$^{-/-}$ mice, we detected no signal at the sarcolemma;

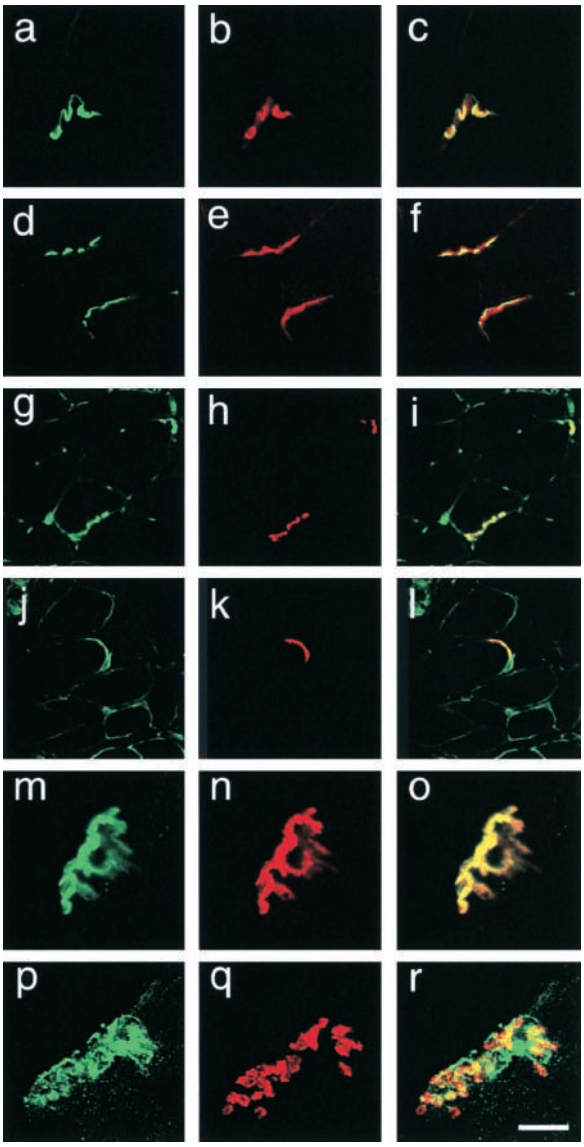

Figure 7. **Aberrant formation of NMJs in regenerating α1syn$^{-/-}$ muscle.** Structure of NMJs in 6-μm cryosections of α1syn$^{-/-}$ (d–f, j–l, and p–r) and wild-type (a–c, g–i, and m–o) TA muscle of untreated mice (a–f), at 7 d (g–l), or three dimensional reconstructed images of NMJ in a single fiber at 8 wk (m–r) after cardiotoxin injection. Specimens are double labeled with antiutrophin antibody (a, d, g, j, m, and p) and Alexa 594–α-BgTx (b, e, h, k, n, and q). The two images are merged to show the relative positions of each molecule (c, f, i, l, o, and r). The mutant mice have remarkably shallow gutters at the NMJs from the early stage of regeneration at 7 d after injection. Moreover, in the mutant mice, the localization of utrophin is not coincident with that of AChR at 8 wk after the treatment. Bar, 20 μm.

however, a trace of putative truncated α1-syntrophin was detected at NMJs (Fig. 8, c and d). Immunohistochemistry showed that β1-syntrophin was overexpressed in fast-type myofibers in the mutant mice (Fig. 8 g). Western blotting analysis confirmed modest up-regulation of β1-syntrophin in the mutant mice (unpublished data). In the regeneration process, the level and expression pattern of β1-syntrophin in mutant muscle was not different from those of wild-type muscle (Fig. 8, f–h). β2-Syntrophin was enriched at NMJs in both wild-type and the mutant muscles, and the expres-

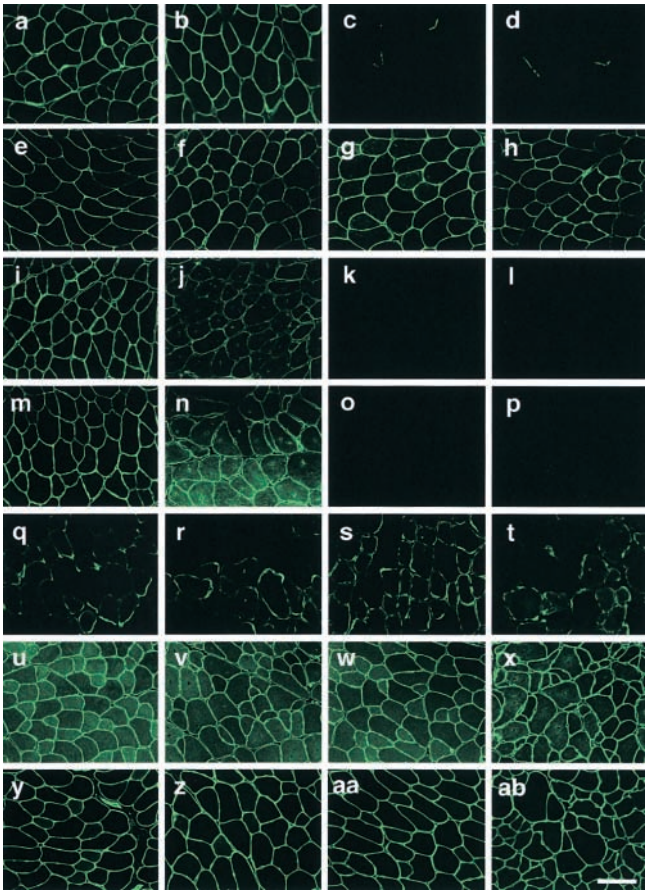

Figure 8. **Expression of α1-syntrophin and its relevant proteins in wild-type and α1syn$^{-/-}$ regenerating muscles.** Expression of α1-syntrophin (a–d), β1-syntrophin (e–h), nNOS (i–l), AQP4 (m–p), VGSCs (q–t), caveolin-3 (u–x), and α-dystrobrevin (y–ab) in TA muscles. Untreated muscle of wild-type (a, e, i, m, q, u, and y) and α1syn$^{-/-}$ mice (c, g, k, o, s, w, and aa). Cardiotoxin-injected muscle of wild-type (b, f, j, n, r, v, and z) and α1syn$^{-/-}$ mice (d, h, l, p, t, x, and ab) at 4 wk after injection. Bar, 50 μm.

sion of β2-syntrophin in regenerating mutant muscle was not different from that of wild-type muscle (unpublished data). Reduced expression of nNOS at the sarcolemma was recognized in a mosaic pattern from 2 wk after injection (Fig. 8 j). However, the expression of nNOS was not detected at the sarcolemma in either treated or untreated muscles of α1syn$^{-/-}$ mice (Fig. 8, k and l). The water channel AQP4 has been reported to be absent at the sarcolemma of α1syn$^{-/-}$ mice (Yokota et al., 2000) and in *mdx* muscle (Frigeri et al., 1998; Liu et al., 1999). AQP4 expression at the sarcolemma started as early as 2 wk after toxin injection in wild-type regenerating muscle (Fig. 8 n). In contrast to the proper localization of AQP4 at the sarcolemma of neonatal α1syn$^{-/-}$ muscle (Yokota et al., 2000), AQP4 expression was completely absent from the sarcolemma in mutant regenerating muscle (Fig. 8 p). An antibody against voltage-gated sodium channel (VGSC) stained NMJs intensely in α1syn$^{-/-}$ and wild-type regenerating muscle as early as 1 wk after cardiotoxin injection (Fig. 8, q–t). Caveolin-3 has been reported to interact with nNOS and modify its enzymatic activity at the sarcolemma (Venema et al., 1997). In regenerating muscles of wild-type and mutant mice, it was normally expressed at the sarcolemma (Fig. 8, v and x). Adams et al. (2000) reported that sarcolemmal expression of α-dystrobrevin-2 was slightly reduced in α1syn$^{-/-}$ muscles. However, our results showed that the expression of α-dystrobrevin in α1syn$^{-/-}$ was indistinguishable from that of wild-type in both regenerating and untreated muscles (Fig. 8, y–ab). By Western blotting analysis, we could not detect any difference between the levels of α-dystrobrevin-1 and -2 in wild-type and in the mutant mice in both conditions (unpublished data).

Discussion

α1syn$^{-/-}$ mice show hypertrophy in muscle regeneration

Regenerating α1syn$^{-/-}$ muscles clearly exhibited extensive hypertrophy from 2 to 8 wk after intramuscular injection of cardiotoxin. Similar hypertrophies of muscle fibers are also seen in α-sarcoglycan–deficient mice (Duclos et al., 1998), dystrophin-utrophin double deficient mice (Deconinck et al., 1997), and *mdx* mice (Coulton et al., 1988), together with reduced specific contractile force. Animal models such as functional overload via synergist ablation can also produce a significant increase in the mass of the overloaded muscles (Timson, 1990). In humans, abnormal muscle hypertrophy is seen in slow twitch skeletal (soleus) muscle of patients with hypertrophic cardiomyopathy (Fananapazir et al., 1993: Lankford et al., 1995), in skeletal muscle in patients with sarcoglycan deficiency (Sewry et al., 1996), and in early stages of DMD (Hardiman, 1994). In the case of hypertrophic cardiomyopathy, which is linked to the *β-myosin heavy chain* gene, the mutated MHCs in slow twitch skeletal muscle have a significant effect on the muscle contractile profile. These hypertrophic processes can be an adaptive response to the decreased contractile force. Interestingly, Lynch et al. (2001) showed that 6–28-mo-old *mdx* mice displayed hypertrophy with normal absolute tetanic force. On the other hand, the absolute tetanic force of 3-mo-old *mdx* muscle is significantly less than that of normal muscle despite the significant hypertrophy (Barton et al., 2002). These observations indicate that the absolute tetanic force of *mdx* increases after 3 mo old, although that of wild-type mice is almost unchanged. In the treated α1syn$^{-/-}$ mice, the absolute tetanic force was significantly less than in the untreated α1syn$^{-/-}$ mice despite the significant hypertrophy. In this point, regenerating muscle of α1syn$^{-/-}$ mice may display a similar situation with 3-mo-old *mdx* muscles. IGF-1 is upregulated in the case of regenerating α1syn$^{-/-}$ muscles (Fig. 5) and in *mdx* mice (De Luca et al., 1999). Interestingly, *mdx* mice showed restoration of tetanic force when hypertrophy was induced by IGF-1 as a transgene, though the specific force of the mice (per area) was not different from that of *mdx* mice (Barton et al., 2002). These reports suggest that IGF-1 can restore the total tetanic force but cannot restore the specific force by inducing hypertrophy.

MHC composition in the regenerating α1syn$^{-/-}$ muscle

Interestingly, the cardiotoxin-injected mutant mice showed a marked deficit in exercise capacity at 7 d compared with the treated wild-type mice. Reduced exercise capacity has also been shown in *mdx* mice by the wire net test. The de-

creased capacity in regenerating α1-syntrophin knockout mice can be, at least partly, explained by the alteration of MHC composition. In the mutant regenerating muscles, the temporal increase of MHC I and IIa has been considerably inhibited and results in a relative increase of MHC IIb expression. A relative decrease of slow components at this period may affect the stamina of mutant mice in the test.

In *mdx* muscle, the reduced contractile force has been explained by the decreases in the proportion of type IIx and increases in type I MHC (Coirault et al., 1999). However, α1-syntrophin knockout mice did not exhibit altered MHC composition at 4–8 wk after the cardiotoxin injection. Actually, we observed predominant hypertrophy of type IIb fibers at the period by immunohistochemistry, whereas glycerol SDS-PAGE did not detect a significant increase of MHC IIb. This suggests that the hypertrophied mutant type IIb fibers contain considerable amounts of MHC IIx, since MHC IIx transcripts are abundant in histochemical type IIb fibers (Smerdu et al., 1994). Therefore, the composition of MHC cannot explain the reduced contractile force in the regeneration period of mutant mice.

Possible mechanisms of the reduction of contractile force in the regenerating α1syn$^{-/-}$ muscle

In *mdx* muscle, deficiency in exercise capacity, reduced contractile force production, and muscle hypertrophy (Coulton et al., 1988; Carter et al., 1995) can be related to the occurrence of many cycles of muscle degeneration and regeneration, membrane fragility, or reduced amount of myofibrils. In contrast, regenerating α1syn$^{-/-}$ TA muscles show no evidence of muscle degeneration, fibrosis, or loss of myofibers (Kameya et al., 1999). In addition, our examination showed no evidence of delay in maturation of myofibers. Therefore, we speculate that abnormal regeneration of syntrophin-null muscle is mainly caused by the lack of functional molecules that interact with α1-syntrophin. We have shown previously that two molecules are lacking from the sarcolemma of α1syn$^{-/-}$ muscle in vivo. First, nNOS was completely absent from the sarcolemma in α1syn$^{-/-}$ muscle (Kameya et al., 1999). Could nNOS be the molecule responsible for the reduction of contractile force in α1syn$^{-/-}$ muscle? NO is widely accepted as a versatile regulator of muscle functions through the cGMP pathway (Kobzik et al., 1994). It has been suggested that NO generated by nNOS at the sarcolemma regulates contraction-stimulated glucose uptake (Roberts et al., 1997) or increases local blood flow in contracting skeletal muscle in part by antagonizing sympathetic vasoconstriction (Thomas et al., 1998). Recently, NO has been reported to protect dystrophin-deficient *mdx* muscle from degeneration when expressed at a high level (Wehling et al., 2001). Moreover, NO can modulate the force–frequency relationship in skeletal muscle (Stamler and Meissner, 2001). However, at least in in vitro studies, NO depletion results in an increase of contractile force (Stamler and Meissner, 2001), whereas α1syn$^{-/-}$ muscle showed the opposite response in the regeneration process. Thus, the loss of nNOS from the sarcolemma may not be directly responsible for the decline in contractile force of the regenerating muscle in the mutant mice. We have shown already that α1-syntrophin plays a major role in recruiting a water channel, AQP4, to the sarcolemma in fast twitch muscle fibers (Yokota et al., 2000). VGSC (Schultz et al., 1998; Gee et al., 1998), stress-activated protein kinase 3 (Hasegawa et al., 1999), and phosphatidylinositol 4,5-bisphosphate (Chockalingam et al., 1999) can also bind to α1-syntrophin. Therefore, it is possible that one or more of these molecules are responsible for the abnormal regeneration, although there is no direct evidence for the involvement of these proteins in contractile force production.

The alternate explanation for this phenomenon is that aberrant NMJs formation in the α1syn$^{-/-}$ mice may affect the force generation of regenerating muscle. Interestingly, a specific force deficit caused not only by atrophy but also by other unknown mechanism(s) exists in skeletal muscle after denervation (Kalliainen et al., 2002).

Finally, proteins involved in excitation-contraction coupling might be responsible for this reduction of contractile property in the mutant regenerating muscle. However, the protein responsible for the deficit in contractile force generation in the mutant mice remains to be determined.

Aberrant formation of NMJs in regenerating TA muscle of α1syn$^{-/-}$

Our results and a previous report (Adams et al., 2000) demonstrated that α1-syntrophin plays an important role in formation of highly organized NMJs both in the developmental process and in muscle regeneration. Since α1-syntrophin is a PDZ protein without any known catalytic domain, the molecules play their roles in NMJ formation by sorting several structural or signaling molecules at the synaptic membrane. Adams et al. (2000) reported that utrophin was severely down-regulated at the NMJs in their α1syn$^{-/-}$ mice, suggesting that α1-syntrophin is an important regulator of utrophin expression at NMJs. It is reasonable to conclude that aberrant NMJs in α1syn$^{-/-}$ muscle are due to the deficiency of utrophin, since utrophin-null muscle showed similar aberrant NMJs to those of α1syn$^{-/-}$ mice (Deconinck et al., 1997; Grady et al., 1997). However, our results showed that the level of utrophin expression is not reduced at the NMJs in the absence of α1-syntrophin in either nonregeneration or regeneration (Fig. 7). This discrepancy in utrophin expression might be derived from a difference in the targeting strategy of the *α1-syntrophin* gene. We inserted an *NEO* gene in the second exon encoding the PDZ domain (Kameya et al., 1999) and later detected a trace of truncated, PDZ-less α1-syntrophin at NMJs (Fig. 8). Ahn and Kunkel (1995) reported that the COOH-terminal fragment conserved among the three syntrophin homologues is sufficient to interact with utrophin. Therefore, it is possible that PDZ-less α1-syntrophin at NMJs recruits utrophin at the sarcolemma. Thus, the most prominent feature of NMJs in α1syn$^{-/-}$ muscle, shallow gutters, is not explained by the lack of utrophin expression. At the same time, we should point out that AChR is not colocalized with utrophin/dystrophin-associated proteins at the NMJs in α1syn$^{-/-}$ muscle on confocal microscopic analysis (Fig. 7). Therefore, α1-syntrophin might play a role in formation of highly organized NMJs by targeting functional molecules other than utrophin at the synaptic membrane. α1-Syntrophin might interact with other PDZ proteins such as membrane-associated guanylate kinase with inverted domain organization-1 (Strochlic et al., 2001), or the molecule

might interact with another class of proteins, one which has a consensus sequence in its COOH-terminal (S/T/V-X-V-COOH) to interact with the PDZ domain, such as ErbB4 (Zhu et al., 1995) or muscle-specific receptor tyrosine kinase (Torres et al., 1998), at NMJs. Aberrant NMJs and deficits in exercise capacity in α1syn$^{-/-}$ mice were observed from an early stage of regeneration. Moreover, the temporal increase of slow muscle components early in the regenerating process might be regulated by the influence of slow nerves. Therefore, aberrant NMJs may be partly responsible for the deficit in exercise capacity of α1syn$^{-/-}$ mice.

The role of α1-syntrophin in skeletal muscle development and regeneration

Is aberrant NMJ formation related to muscle hypertrophy and/or reduced contractile force in the regeneration process? Mutant skeletal muscle showed neither hypertrophy nor reduced contractile force in the developmental stage without cardiotoxin treatment, although they do have aberrant NMJs. However, in regeneration hypertrophy becomes apparent 2 wk after toxin treatment, and the shallower synaptic gutter and enlargement of NMJs became more apparent at 4–8 wk after cardiotoxin treatment in α1syn$^{-/-}$ muscles (unpublished data). This disparity between developmental stage and regeneration process in α1syn$^{-/-}$ mice may be caused by the difference of expression patterns of α1-syntrophin and its associated factors between developmental and regeneration processes. AQP4 is abundantly expressed in the neonatal stage without accompanying expression of α1-syntrophin (Yokota et al., 2000), but it is not expressed until later in the regeneration process as shown in this study. AQP4 may not be related directly to hypertrophy and reduced contractile force in the regeneration process of α1syn$^{-/-}$ mice, but other molecules can show the same pattern of expression and explain the peculiar phenomenon. Accordingly, α1-syntrophin and its related molecules may have a particular role in regeneration, rather than in development, of skeletal muscle.

Muscular dystrophy and muscle hypertrophy

The primary absence of dystrophin is accompanied by a secondary deficiency of several dystrophin-associated molecules, including α- and β-dystroglycans, sarcoglycans, sarcospan, syntrophins, and dystrobrevins, from the sarcolemma (Ozawa et al., 1995). Therefore, molecular dissection of associated molecules by gene targeting is a powerful tool to clarify the molecular pathogenesis of muscular dystrophy. In particular, the expression of dystrophin-associated proteins other than nNOS is well preserved in α1syn$^{-/-}$ mice; therefore, the mutant mice are a good model to examine the functions of α1-syntrophin and its own downstream elements both in physiological and pathological conditions. In the present study, we clearly demonstrated that α1-syntrophin plays an important role in muscle regeneration: in the absence of α1-syntrophin, regenerating muscle showed a marked decrease in the exercise capacity and contractile force and an increase in muscle hypertrophy and aberrant NMJ formation. DMD patients and all dystrophin-deficient models (dogs, cats, and mice) pass through an early phase of muscle hypertrophy to some extent (Partridge, 1991). The deficit caused by the lack of α1-syntrophin may largely account for the phenomenon found in the early regeneration stage of DMD.

Materials and methods

Animals

8-week-old α1syn$^{-/-}$ (Kameya et al., 1999) and wild-type littermates were used in this study. The animals were allowed ad libitum access to food and drinking water. Mice carrying mutations were identified by Southern blot analysis as described (Kameya et al., 1999).

Cardiotoxin injection and tissue preparation

0.1 ml of 10 μM cardiotoxin (Wako Pure Chemical Industries) in 0.9% saline was injected directly into the right TA muscle with a 27-gauge needle under ether anesthesia. Mice were killed by cervical dislocation, and the cardiotoxin-injected TA muscles (right) and noninjected contralateral TA muscles (left) were removed for analysis at 1, 3, and 5 d, and 1, 2, 4, 8, 12, and 24 wk after injection. Body weight and wet muscle weight (TA) were measured. Several of the muscles were frozen in isopentane cooled by liquid nitrogen for histological, immunohistochemical analysis, and the other muscles were frozen directly in liquid nitrogen for RNA isolation, and stored at −80°C.

Hematoxylin and eosin staining

10-μm cryosections were cut in the middle part of the muscle belly to obtain the largest CSA, placed on poly-L-lysine–coated slides, air dried, and stained with hematoxylin and eosin. The sections were viewed and photographed using an HC-2500 digital camera system™ (Fuji Photo Film Co., Ltd.).

Single muscle fiber isolation

We isolated single muscle fibers according to the method described previously (Rosenblatt et al., 1995) with a simple modification. In brief, the TA muscle was rinsed in PBS, put into a Petri dish containing 0.5% type I collagenase (Worthington Biochemical Corp.) in DME (Invitrogen), and incubated at 37°C for 1.5–3 h.

Immunohistochemical analysis

Antibodies. Monoclonal antibodies BF-B6, BA-D5, or BF-F3 obtained from DSM (Deutsche Sammlung von Mikroorganismen und Zellkulturen Abt. Menschliche und Tierische Zellkulturen) detect neonatal type MHC, MHC I, or MHC IIb, respectively. Monoclonal antibody SC-71 (DSM) strongly labels MHC IIa and labels MHC IIx to a lesser extent. We concluded that the fibers negative for BA-D5, BF-F3, and SC-71 antibodies were type IIx. The following polyclonal antibodies were used for immunofluorescence: anti–α1-syntrophin (Asahi Techno Glass Co., Ltd.), anti-myogenin (Santa Cruz Biotechnology, Inc.), anti–Myf-5 (Santa Cruz Biotechnology, Inc.), anti–Myf-6 (Santa Cruz Biotechnology, Inc.), anti-MyoD (Santa Cruz Biotechnology, Inc.), antiutrophin (Imamura and Ozawa, 1998), anti–caveolin-3 (Asahi Techno Glass Co., Ltd.), anti-NOS1 (Santa Cruz Biotechnology, Inc.), anti–sodium channel (III-IV Linker Region) (Upstate Biotechnology), and anti–α-dystrobrevin-1 and -2 (Yoshida et al., 2000). Human β1-syntrophin (195–378 a.a.) was fused to GST in the pGEX vector (Amersham Biosciences) and maltose-binding protein in the pMAL-c2 vector (New England Biolabs, Inc.). The GST fusion β1-syntrophin protein was used as an antigen. Obtained rabbit antiserum was purified with the affinity column coupled with the maltose-binding protein–β1-syntrophin fusion protein. The last 43 amino acids of mouse AQP4 were fused to GST in the pGET−1λT vector (Amersham Biosciences), and the recombinant proteins were purified and used to obtain rabbit polyclonal antibodies.

Immunofluorescence. Acetone-fixed cryosections (6 μm) were blocked with 5% goat serum and 2% BSA in PBS and then incubated with primary antibody at 4°C overnight. 4% paraformaldehyde-fixed single muscle fibers were blocked with 20% goat serum in PBS and then incubated with a primary antibody in 0.35% carrageenan in PBS at 4°C overnight. FITC-conjugated anti–rabbit goat antibody (Biosource International) or Alexa 488–labeled goat anti–rabbit IgG (H+L) (Molecular Probes) was used as the secondary antibody. To identify NMJs, AChRs were detected with Alexa 594–labeled α-BgTx (Molecular Probes). The sections were viewed and photographed by a laser scanning microscope, FLUOVIEW™ (Olympus). Z serial images were collected from whole-mount single fiber samples with a 63× oil objective using TCSSP™ (Leica). A single projected image was created by overlaying each set of z series images.

Northern blot analysis of IGF-1

A First-Strand cDNA Synthesis kit™ (Amersham Biosciences) was used to synthesize first strand cDNA from total RNA isolated from TA muscles of wild-type mice. IGF-1 cDNA was amplified by PCR using two oligonucleotide primers (5′-GTCTTCACACCTCTTCTACC-3′ and 5′-CCTTCTGAGTCTTGGGCATGTCAG-3′). A 320-base pair PCR product covering exon 3 and part of exon 4 of the IGF-1 gene was cloned into a pCR^R 2.1 vector (Invitrogen) and confirmed by sequencing using a DNA analysis system LIC-4200L-2™ (LI-COR, Inc.). Glyceraldehyde-3-phosphate dehydrogenase (G3PDH) cDNA was amplified using RT-PCR Control Amplimer Set™ (CLONTECH Laboratories, Inc.) and cloned as described above. The cDNA fragment was digested with EcoRI (TaKaRa Shuzo Co., Ltd.) and labeled with ^{32}P using a Random Primer DNA Labeling kit version 2™ (TaKaRa Shuzo Co., Ltd.). Total RNA was prepared from TA muscles by using RNAzol™ B (TEL-TEST, Inc.). 30 μg of total RNA was electrophoresed on a 1.0% denaturing agarose-formaldehyde gel, transferred to Hybond N$^+$ nylon membrane™ (Amersham Biosciences) and heated at 80°C for 2 h. The hybridization was performed using ^{32}P-labeled DNA probes. Prehybridization (30 min) and hybridization (overnight) were performed at 42°C in ULTRAhyb™ hybridization buffer (Ambion). Washing was performed for 2 × 5 min at 42°C with 2 × SSC and 0.1% SDS, 2 × 15 min at 42°C with 0.1 × SSC and 0.1% SDS. The hybridized probe was detected and quantified using the Bio-Imaging analyzer BAS-2500™ (Fuji Photo Film Co., Ltd.).

Measurement of fiber CSA

The CSA of each fiber classified by the expression of MHC was measured using a Mac SCOPE™ (Mitani Co.). We measured fiber CSA on the sections from three muscles in each group (noninjected and cardiotoxin-injected wild-type and α1syn$^{-/-}$ mice). A total of 200 fiber profiles were measured in the predetermined area of TA muscles. All fiber profiles traced in each group of muscles were pooled and plotted for their size distribution according to percent frequency.

Wire net holding test

The untreated male mice of 8-wk-old wild-type ($n = 3$) and α1syn$^{-/-}$ ($n = 3$) or the mice at 7 d–8 wk after cardiotoxin injection into TA muscles of hind legs of 8-wk-old wild-type ($n = 13$) and α1syn$^{-/-}$ ($n = 8$) were examined. The mice were placed on a fine wire net. Then, the net was slowly turned over. The time until the mouse fell off was measured up to a maximum time of 300 s.

MHC isoform separation

The muscles frozen in isopentane cooled by liquid nitrogen were homogenized and extracted on ice for 60 min in 4 vol of buffer (pH 6.5) as described previously (Butler-Browne and Whalen, 1984). MHC separation on polyacrylamide gels containing 30% glycerol was performed according to the methods described previously (Agbulut et al., 1996) with simple modification. In brief, mini gels were made in the mini protein III Dual slab cell system (Bio-Rad Laboratories Inc.). 0.5 μg of total protein was run on each well. The upper buffer contained 10 mM of 2-mercaptoethanol. During electrophoresis, the temperature of the buffer was maintained at 5°C. After migration, the gels were silver stained using 2D-Silver Stain II "Daiichi" (Daiichi Pure Chemicals Co., Ltd.). The image was scanned and then analyzed using Lumi-Imager F1 software (Hoffmann-La Roche, Inc.).

Muscle physiology

Tetanic force and isometric twitch force of TA muscles were measured as described previously (Xiao et al., 2000). The entire TA was removed with its tibial origin intact, and the distal portion of the TA tendon and its origin were secured with a 5–0 silk suture. The TA was mounted in a vertical tissue chamber and was connected to a force transducer UL-50GR (Microtech) and length servosystem (Shimazu). Electrical stimulation using a SEN3301 (Nihon Kohden) was applied through a pair of platinum wires placed on both sides of the muscle in physiological soft solution (150 mM NaCl, 4 mM KCl, 2 mM $CaCl_2$, 1 mM $MgCl_2$, 5.6 mM glucose, 5 mM Hepes, pH 7.4, 0.02 mM D-tubocurarine). The TA was positioned midway between the two electrodes. Muscle fiber length was adjusted incrementally by using a micropositioner until peak isometric twitch force (Pt) responses were obtained (i.e., optimal fiber length [L0]). The dependence of force generation on the rate of stimulation and maximum tetanic force (P0) was assessed by use of a range of stimulation frequencies (20, 50, 75, and 100 pulses per second) delivered in 500-ms duration trains with 2 min intervening between each train. After these measurements, the stimulated muscle was dried and weighed after tendon and bone attachments were removed. All forces were normalized for a dried CSA, the latter estimated on the basis of the following formula: dried muscle weight (in milligrams)/[L0 (in millimeters) × 1.056 (in milligrams per cubic millimeter)]. The estimated CSA was used to determine specific twitch forces (Pt/CSA) and specific tetanic forces (P0/CSA) of the muscles.

Statistical analysis

The relative weight of muscle, the number of myofibers and the expression of IGF-1 mRNA, the holding time on the wire net holding test, and the levels of MHC protein isoforms between wild-type and α1syn$^{-/-}$, noninjected and cardiotoxin-injected muscle were compared using Student's t test. CSA distributions and mean fiber CSA were compared using F test and Student's or Welch's t test. $P < 0.05$ was considered statistically significant.

The authors thank Reiko Shimoda and all members of the Department of Molecular Therapy for technical assistance and discussion.

This work was supported by grants for Health Science Research for the Center of Excellence program, Human Frontier Science Program, Research on Nervous and Mental Disorders (10B, 13-B) from the Ministry of Health and Welfare, and Grant-in Aids for Scientific Research (11170264) from the Ministry of Education, Culture, Sports, Science and Technology of Japan.

Submitted: 15 April 2002
Revised: 2 August 2002
Accepted: 5 August 2002

References

Adams, M.E., M.H. Butler, T.M. Dwyer, M.F. Peters, A.A. Murnane, and S.C. Froehner. 1993. Two forms of mouse syntrophin, a 58 kd dystrophin-associated protein, differ in primary structure and tissue distribution. *Neuron.* 11:531–540.

Adams, M.E., T.M. Dwyer, L.L. Dowler, R.A. White, and S.C. Froehner. 1995. Mouse alpha 1- and beta 2-syntrophin gene structure, chromosome localization, and homology with a discs large domain. *J. Biol. Chem.* 270:25859–25865.

Adams, M.E., N. Kramarcy, S.P. Krall, S.G. Rossi, R.L. Rotundo, R. Sealock, and S.C. Froehner. 2000. Absence of alpha-syntrophin leads to structurally aberrant neuromuscular synapses deficient in utrophin. *J. Cell Biol.* 150:1385–1398.

Agbulut, O., Z. Li, V. Mouly, and G.S. Butler-Browne. 1996. Analysis of skeletal and cardiac muscle from desmin knock-out and normal mice by high resolution separation of myosin heavy-chain isoforms. *Biol. Cell.* 88:131–135.

Ahn, A.H., and L.M. Kunkel. 1995. Syntrophin binds to an alternatively spliced exon of dystrophin. *J. Cell Biol.* 128:363–371.

Ahn, A.H., M. Yoshida, M.S. Anderson, C.A. Feener, S. Selig, Y. Hagiwara, E. Ozawa, and L.M. Kunkel. 1994. Cloning of human basic A1, a distinct 59-kDa dystrophin-associated protein encoded on chromosome 8q23-24. *Proc. Natl. Acad. Sci. USA.* 91:4446–4450.

Barton, E.R., L. Morris, A. Musaro, N. Rosenthal, and H.L. Sweeney. 2002. Muscle-specific expression of insulin-like growth factor I counters muscle decline in *mdx* mice. *J. Cell Biol.* 157:137–148.

Brenman, J.E., D.S. Chao, S.H. Gee, A.W. McGee, S.E. Craven, D.R. Santillano, Z. Wu, F. Huang, H. Xia, M.F. Peters, et al. 1996. Interaction of nitric oxide synthase with the postsynaptic density protein PSD-95 and alpha1-syntrophin mediated by PDZ domains. *Cell.* 84:757–767.

Butler-Browne, G.S., and R.G. Whalen. 1984. Myosin isozyme transitions occurring during the postnatal development of the rat soleus muscle. *Dev. Biol.* 102:324–334.

Byers, T.J., L.M. Kunkel, and S.C. Watkins. 1991. The subcellular distribution of dystrophin in mouse skeletal, cardiac, and smooth muscle. *J. Cell Biol.* 115: 411–421.

Cartaud, A., F. Stetzkowski-Marden, and J. Cartaud. 1993. Identification of dystrophin-binding protein(s) in membranes from Torpedo electrocyte and rat muscle. *J. Biol. Chem.* 268:13019–13022.

Carter, G.T., M.A. Wineinger, S.A. Walsh, S.J. Horasek, R.T. Abresch, and W.M. Fowler, Jr. 1995. Effect of voluntary wheel-running exercise on muscles of the mdx mouse. *Neuromuscul. Disord.* 5:323–332.

Chockalingam, P.S., S.H. Gee, and H.W. Jarrett. 1999. Pleckstrin homology domain 1 of mouse alpha 1-syntrophin binds phosphatidylinositol 4,5-bisphosphate. *Biochemistry.* 38:5596–5602.

Coirault, C., F. Lambert, S. Marchand-Adam, P. Attal, D. Chemla, and Y. Lecarpentier. 1999. Myosin molecular motor dysfunction in dystrophic mouse diaphragm. *Am. J. Physiol.* 277:C1170–C1176.

Coulton, G.R., N.A. Curtin, J.E. Morgan, and T.A. Partridge. 1988. The mdx

mouse skeletal muscle myopathy: II. Contractile properties. *Neuropathol. Appl. Neurobiol.* 14:299–314.

Cullen, M.J. 1997. Muscle regeneration. *In* Dystrophin. S.S. Brown, and J.A. Lucy, editors. Cambridge University Press, Cambridge, UK. 233–273.

Deconinck, A.E., A.C. Potter, J.M. Tinsley, S.J. Wood, R. Vater, C. Young, L. Metzinger, A. Vincent, C.R. Slater, and K.E. Davies. 1997. Postsynaptic abnormalities at the neuromuscular junctions of utrophin-deficient mice. *J. Cell Biol.* 136:883–894.

De Luca, A., S. Pierno, C. Camerino, D. Cocchi, and D.C. Camerino. 1999. Higher content of insulin-like growth factor-I in dystrophic *mdx* mouse: potential role in the spontaneous regeneration through an electrophysiological investigation of muscle function. *Neuromuscul. Disord.* 9:11–18.

Duclos, F., V. Straub, S.A. Moore, D.P. Venzke, R.F. Hrstka, R.H. Crosbie, M. Durbeej, C.S. Lebakken, A.J. Ettinger, J. van der Meulen, et al. 1998. Progressive muscular dystrophy in alpha-sarcoglycan–deficient mice. *J. Cell Biol.* 142:1461–1471.

Fananapazir, L., M.C. Dalakas, F. Cyran, G. Cohn, and N.D. Epstein. 1993. Missense mutations in the beta-myosin heavy-chain gene cause central core disease in hypertrophic cardiomyopathy. *Proc. Natl. Acad. Sci. USA.* 90:3993–3997.

Frigeri, A., G.P. Nicchia, J.M. Verbavatz, G. Valenti, and M. Svelto. 1998. Expression of aquaporin-4 in fast-twitch fibers of mammalian skeletal muscle. *J. Clin. Invest.* 102:695–703.

Gee, S.H., R. Madhavan, S.R. Levinson, J.H. Caldwell, R. Sealock, and S.C. Froehner. 1998. Interaction of muscle and brain sodium channels with multiple members of the syntrophin family of dystrophin-associated proteins. *J. Neurosci.* 18:128–137.

Grady, R.M., J.P. Merlie, and J.R. Sanes. 1997. Subtle neuromuscular defects in utrophin-deficient mice. *J. Cell Biol.* 136:871–882.

Hardiman, O. 1994. Dystrophin deficiency, altered cell signalling and fibre hypertrophy. *Neuromuscul. Disord.* 4:305–315.

Hasegawa, M., A. Cuenda, M.G. Spillantini, G.M. Thomas, V. Buee-Scherrer, P. Cohen, and M. Goedert. 1999. Stress-activated protein kinase-3 interacts with the PDZ domain of alpha1-syntrophin. A mechanism for specific substrate recognition. *J. Biol. Chem.* 274:12626–12631.

Imamura, M., and E. Ozawa. 1998. Differential expression of dystrophin isoforms and utrophin during dibutyryl-cAMP-induced morphological differentiation of rat brain astrocytes. *Proc. Natl. Acad. Sci. USA.* 95:6139–6144.

Kalliainen, L.K., S.S. Jejurikar, L.W. Liang, M.G. Urbanchek, and W.M. Kuzon, Jr. 2002. A specific force deficit exists in skeletal muscle after partial denervation. *Muscle Nerve.* 25:31–38.

Kameya, S., Y. Miyagoe, I. Nonaka, T. Ikemoto, M. Endo, K. Hanaoka, Y. Nabeshima, and S. Takeda. 1999. Alpha1-syntrophin gene disruption results in the absence of neuronal-type nitric-oxide synthase at the sarcolemma but does not induce muscle degeneration. *J. Biol. Chem.* 274:2193–2200.

Kobzik, L., M.B. Reid, D.S. Bredt, and J.S. Stamler. 1994. Nitric oxide in skeletal muscle. *Nature.* 372:546–548.

Kramarcy, N.R., A. Vidal, S.C. Froehner, and R. Sealock. 1994. Association of utrophin and multiple dystrophin short forms with the mammalian M(r) 58,000 dystrophin-associated protein (syntrophin). *J. Biol. Chem.* 269: 2870–2876.

Lankford, E.B., N.D. Epstein, L. Fananapazir, and H.L. Sweeney. 1995. Abnormal contractile properties of muscle fibers expressing beta-myosin heavy chain gene mutations in patients with hypertrophic cardiomyopathy. *J. Clin. Invest.* 95:1409–1414.

Liu, J.W., Y. Wakayama, M. Inoue, S. Shibuya, H. Kojima, T. Jimi, and H. Oniki. 1999. Immunocytochemical studies of aquaporin 4 in the skeletal muscle of mdx mouse. *J. Neurol. Sci.* 164:24–28.

Lynch, G.S., R.T. Hinkle, J.S. Chamberlain, S.V. Brooks, and J.A. Faulkner. 2001. Force and power output of fast and slow skeletal muscles from *mdx* mice 6-28 months old. *J. Physiol.* 535:591–600.

Ozawa, E., M. Yoshida, A. Suzuki, Y. Mizuno, Y. Hagiwara, and S. Noguchi. 1995. Dystrophin-associated proteins in muscular dystrophy. *Hum. Mol. Genet.* 4:1711–1716.

Partridge, T. 1991. Animal models of muscular dystrophy–what can they teach us? *Neuropathol. Appl. Neurobiol.* 17:353–363.

Peters, M.F., M.E. Adams, and S.C. Froehner. 1997. Differential association of syntrophin pairs with the dystrophin complex. *J. Cell Biol.* 138:81–93.

Piluso, G., M. Mirabella, E. Ricci, A. Belsito, C. Abbondanza, S. Servidei, A.A. Puca, P. Tonali, G.A. Puca, and V. Nigro. 2000. Gamma1- and gamma2-syntrophins, two novel dystrophin-binding proteins localized in neuronal cells. *J. Biol. Chem.* 275:15851–15860.

Roberts, C.K., R.J. Barnard, S.H. Scheck, and T.W. Balon. 1997. Exercise-stimulated glucose transport in skeletal muscle is nitric oxide dependent. *Am. J. Physiol.* 273:E220–E225.

Rosenblatt, J.D., A.I. Lunt, D.J. Parry, and T.A. Partridge. 1995. Culturing satellite cells from living single muscle fiber explant. *In Vitro Cell. Dev. Biol. Anim.* 31:773–779.

Schultz, J., U. Hoffmuller, G. Krause, J. Ashurst, M.J. Macias, P. Schmieder, J. Schneider-Mergener, and H. Oschkinat. 1998. Specific interactions between the syntrophin PDZ domain and voltage-gated sodium channels. *Nat. Struct. Biol.* 5:19–24.

Sealock, R., M.H. Butler, N.R. Kramarcy, K.X. Gao, A.A. Murnane, K. Douville, and S.C. Froehner. 1991. Localization of dystrophin relative to acetylcholine receptor domains in electric tissue and adult and cultured skeletal muscle. *J. Cell Biol.* 113:1133–1144.

Sewry, C.A., J. Taylor, L.V. Anderson, E. Ozawa, R. Pogue, F. Piccolo, K. Bushby, V. Dubowitz, and F. Muntoni. 1996. Abnormalities in alpha-, beta- and gamma-sarcoglycan in patients with limb-girdle muscular dystrophy. *Neuromuscul. Disord.* 6:467–474.

Smerdu, V., I. Karsch-Mizrachi, M. Campione, L. Leinwand, and S. Schiaffino. 1994. Type IIx myosin heavy chain transcripts are expressed in type IIb fibers of human skeletal muscle. *Am J Physiol.* 267:C1723–C1728.

Stamler, J., and G. Meissner. 2001. Physiology of nitric oxide in skeletal muscle. *Physiol. Rev.* 81:209–233.

Strochlic, L., A. Cartaud, V. Labas, W. Hoch, J. Rossier, and J. Cartaud. 2001. MAGI-1c: a synaptic MAGUK interacting with MuSK at the vertebrate neuromuscular junction. *J. Cell Biol.* 153:1127–1132.

Suzuki, A., M. Yoshida, and E. Ozawa. 1995. Mammalian alpha 1- and beta 1-syntrophin bind to the alternative splice-prone region of the dystrophin COOH terminus. *J. Cell Biol.* 128:373–381.

Thomas, G.D., M. Sander, K.S. Lau, P.L. Huang, J.T. Stull, and R.G. Victor. 1998. Impaired metabolic modulation of alpha-adrenergic vasoconstriction in dystrophin-deficient skeletal muscle. *Proc. Natl. Acad. Sci. USA.* 95: 15090–15095.

Timson, B.F. 1990. Evaluation of animal models for the study of exercise-induced muscle enlargement. *J. Appl. Physiol.* 69:1935–1945.

Torres, R., B.L. Firestein, H. Dong, J. Staudinger, E.N. Olson, R.L. Huganir, D.S. Bredt, N.W. Gale, and G.D. Yancopoulos. 1998. PDZ proteins bind, cluster, and synaptically colocalize with Eph receptors and their ephrin ligands. *Neuron.* 21:1453–1463.

Venema, V.J., H. Ju, R. Zou, and R.C. Venema. 1997. Interaction of neuronal nitric-oxide synthase with caveolin-3 in skeletal muscle. Identification of a novel caveolin scaffolding/inhibitory domain. *J. Biol. Chem.* 272:28187–28190.

Wehling, M., M.J. Spencer, and J.G. Tidball. 2001. A nitric oxide synthase transgene ameliorates muscular dystrophy in mdx mice. *J. Cell Biol.* 155:123–131.

Xiao, X., J. Li, Y. Tsao, D. Dressman, E.P. Hoffman, and J.F. Wachko. 2000. Full functional rescue of a complete muscle (TA) in dystrophic hamsters by adeno-associated virus vector-directed gene therapy. *J. Virol.* 74:1436–1442.

Yang, B., D. Jung, J.A. Rafael, J.S. Chamberlain, and K.P. Campbell. 1995. Identification of alpha-syntrophin binding to syntrophin triplet, dystrophin, and utrophin. *J. Biol. Chem.* 270:4975–4978.

Yokota, T., Y. Miyagoe, Y. Hosaka, K. Tsukita, S. Kameya, S. Shibuya, R. Matsuda, Y. Wakayama, and S. Takeda. 2000. Aquaporin-4 is absent at the sarcolemma and at perivascular astrocyte endfeet in α1-syntrophin knockout mice. *Proc. Japan Acad.* 76:22–27.

Yoshida, M., H. Hama, M. Ishikawa-Sakurai, M. Imamura, Y. Mizuno, K. Araishi, E. Wakabayashi-Takai, S. Noguchi, T. Sasaoka, and E. Ozawa. 2000. Biochemical evidence for association of dystrobrevin with the sarcoglycan-sarcospan complex as a basis for understanding sarcoglycanopathy. *Hum. Mol. Genet.* 9:1033–1040.

Zhu, X., C. Lai, S. Thomas, and S.J. Burden. 1995. Neuregulin receptors, erbB3 and erbB4, are localized at neuromuscular synapses. *EMBO J.* 14:5842–5848.